THE ASTROPHYSICAL JOURNAL, Vol. 151, February 1968

ANALYSIS OF F AND G SUBDWARFS. II. A MODEL-ATMOSPHERE ABUNDANCE ANALYSIS OF THE SUBDWARFS HD 140283 AND HD 19445

JUDITH G. COHEN AND STEPHEN E. STROM
Smithsonian Astrophysical Observatory and Harvard College Observatory, Cambridge, Massachusetts
Received April 25, 1967; revised August 9, 1967

ABSTRACT

A grid of model atmospheres has been used to perform an abundance analysis of these two extreme Population II stars

The abundances determined from the models confirm the general results of previous investigations, namely that metals are deficient by a factor of about 100 relative to average Population I abundances. A marginal deficiency of *s*-process material relative to the average deficiency is found; the carbon deficiencies are comparable to those of the other elements and for HD 19445 the α-process elements are enhanced From the analysis it also appears that convection plays a significant role in determining the temperature structure of subdwarf atmospheres.

I. INTRODUCTION

The positions of HD 19445 and HD 140283 in the H-R diagram were discussed in Paper I (Strom, Cohen, and Strom 1966). Despite the large uncertainty in the ages of these subdwarfs brought about by their small parallaxes and the intrinsic uncertainties in the stellar models, it seems safe to say that both stars are extremely old ($\sim 10^{10}$ years). Consequently, their element abundances should provide information concerning the chemical abundances at the earliest stages of galactic evolution. Owing to the extreme weak-line character of their spectra and the hope of answering basic cosmogonical questions, these stars have been the object of extensive spectrophotometric investigation.

Previous abundance analyses of HD 19445 have been made by Chamberlain and Aller (1951) and Aller and Greenstein (1960). HD 140283 has been analyzed by Chamberlain and Aller (1951), Aller and Greenstein (1960), and Baschek (1959, 1962). Only Baschek attempts the use of a model atmosphere in his analysis, and even in this case, owing to the lack of adequate photometric data, he chose the wrong parameters for his models. With more modern techniques for model choice and abundance analysis at our disposal, we can hope to improve on these previously reported results.

In Paper I we have discussed the choice of the range of $T_{\rm eff}$ for these two stars based on spectrum scans and Hγ profiles. Before we can specify the grid of models to be used in the analysis, we must choose representative values for the surface gravity. If we use Faulkner and Iben's (1966) evolutionary tracks as a guide, we can compute values of $\log g$, given $T_{\rm eff}$ and $(L/L_\odot)$. Since the two stars have almost identical values of these quantities they must have the same surface gravity if their helium content is the same. From the evolutionary tracks shown in Paper I we obtain $\log g = 4.1 \pm 0.3$ for the $Y = 0.10$ track, and $\log g = 3.7 \pm 0.3$ for $Y = 0.35$.

In principle it is also possible to obtain a value of the surface gravity from the spectrum scans since in the $T_{\rm eff}$ range 5000°–6000° K the size of the Balmer discontinuity is a measure of the surface gravity.

Unfortunately, two effects prevent us from obtaining accurate values of surface gravity through measurement of the Balmer discontinuity. First, the uncertainty in the calibration of the primary spectrophotometric standard, Vega, amounts to approximately 0.05 mag for $\lambda < 3650$ Å. Second, the effects of departures from LTE is to re-

duce the Balmer discontinuity by up to 0.10 mag depending on the choice of reaction rate for associative detachment of H^- (Strom 1967). With these errors in mind, we quote below the values of log g deduced from LTE models and from the scans of Oke (1965) and Melbourne (1960):

$$\text{HD } 19445: \log g = 4.0 \pm 0.5,$$

$$\text{HD } 140283: \log g = 3.5 \pm 0.5.$$

That these values are not inconsistent with the values deduced from stellar models is at least mildly encouraging.

II. CHOICE OF MODEL ATMOSPHERE

Keeping in mind the range in values of log g discussed in § I and the T_{eff} values deduced in Paper I, we chose as our starting models those summarized in Table 1.

TABLE 1

INITIAL MODELS

Star	Model I
HD 140283	(5500, 3.7, 0.01, 0)
HD 19445	(5500, 4.0, 0.01, 0)

TABLE 2

IRON ABUNDANCES FROM INITIAL MODELS

Star	Fe I	Fe II
HD 140283	−7.72±0.15	−7.28±0.24
HD 19445	−7.56±0.20	−7.67±0.15

The system for designating models is (T_{eff}, log g, metal content, v_t). The entry 0.01 for metal content indicates that the values obtained by Goldberg, Müller, and Aller (1960; hereinafter cited as GMA values) for solar metal abundances have been divided by 100; v_t is microturbulent velocity. We chose $v_t = 0$ since previous works (Aller and Greenstein 1960; Wallerstein 1962) suggest small values for the microturbulent velocity parameter.

If our choice of T_{eff}, log g, and v_t is correct, the model should result in our predicting: (*a*) consistent abundances from separate ionization states of a given element; (*b*) no systematic variation of deduced abundance with lower excitation potential (if there are no non-LTE effects or systematic errors in the transition probabilities); and (*c*) no systematic variation of deduced abundance with line strength; such variations would be expected if an inappropriate value of v_t were chosen.

In Table 2 we summarize the logarithmic abundance ratios (Fe I/H) and (Fe II/H) in these two stars deduced by using the above models. The results for HD 140283 suggest that a lower surface gravity or higher temperature is required in order to make the abundances agree for the two ionization states.

In Figures 1*a* and 1*b* we plot for both stars the abundances deduced for Fe I lines as a function of lower excitation potential. For HD 140283, the low abundances computed for the values of $\chi \approx 3$ eV suggest that either the temperature or the amount of Fe I relative to Fe II computed for the models is too high where these lines are formed. The adjoining plot for HD 19445 shows relatively consistent abundances for all χ.

In Figures 2*a* and 2*b* we plot for both stars the calculated abundances against the ob-

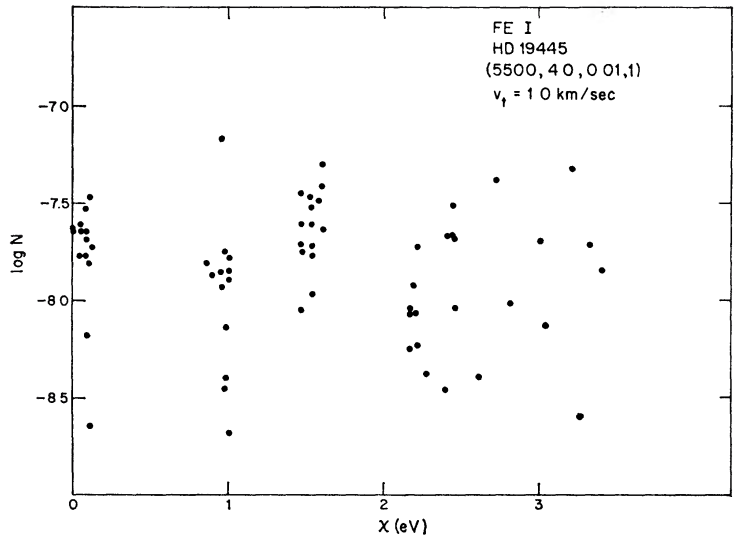

FIG. 1*a*.—Deduced abundance as a function of the lower excitation potential for Fe I lines in HD 19445 using the model (5500, 4 0, 0 01, 1).

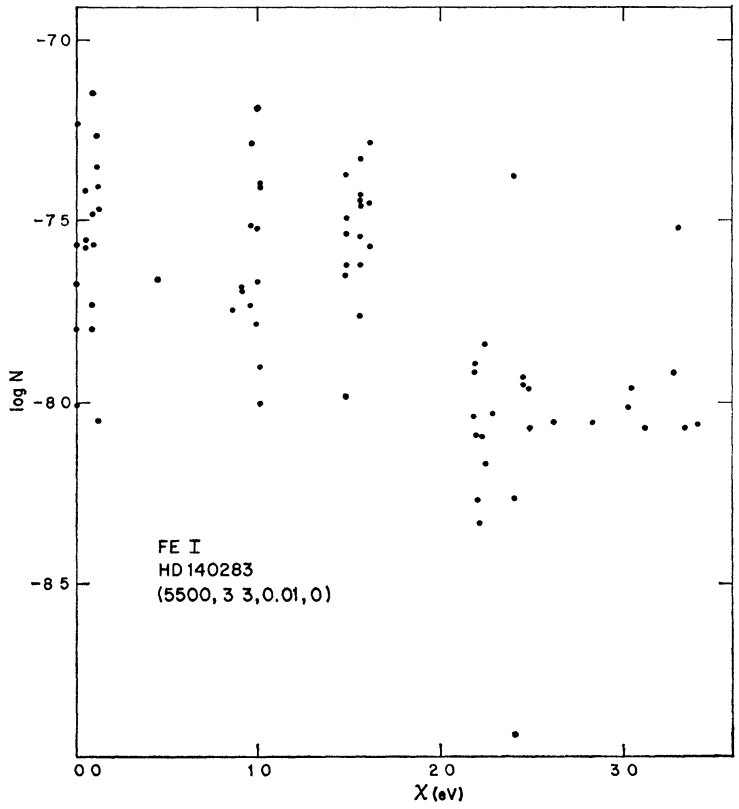

FIG. 1*b*.—Deduced abundance as a function of the lower excitation potential for Fe I lines in HD 140283 using the model (5500, 3 3, 0.01, 0).

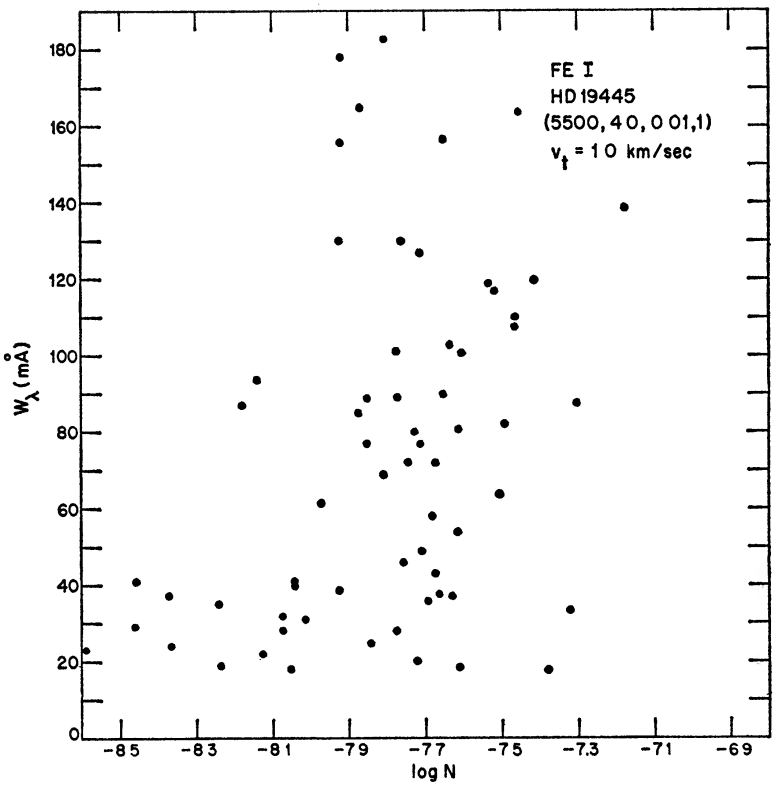

FIG. 2*a*.—Deduced abundance as a function of equivalent width for Fe I lines in HD 19445 using the model (5500, 4.0, 0.01, 1).

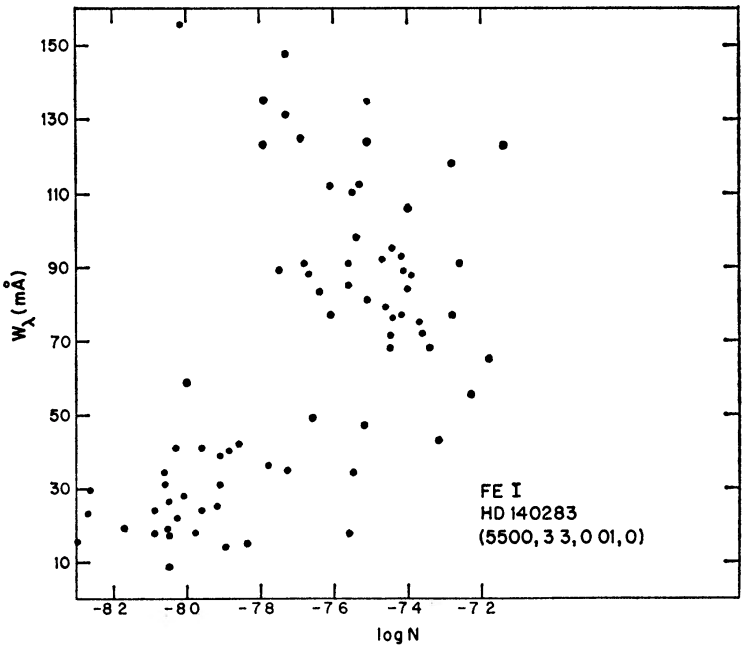

FIG. 2*b*.—Deduced abundance as a function of equivalent width for Fe I lines in HD 140283 using the model (5500, 3.3, 0.01, 0).

served equivalent width of the Fe I lines. In each case the strong lines predict a larger abundance than the weak lines. We interpret this by noting that too low a value of v_t leads us to choose too high a value of abundance for lines that fall on the flat portion of the curve of growth. This suggests that v_t must be increased in our next choice of model.

In Figure 3 we see a choice of $T_{\rm eff} = 6000°$ for HD 19445 leads to an overpopulation of the high-excitation states. Figure 4 demonstrates that microturbulent velocity $v_t =$ 2.5 km/sec is too large for this star. In Tables 3 and 4 we present the Fe I and Fe II abundances computed for the indicated models.

It is apparent that a model having (5750, 4.0, 0.01, 1–2) would best fit the HD 19445 model, whereas for HD 140283 it is almost impossible to deduce a model that will predict an entirely consistent behavior for the deduced abundances. The best value of log g

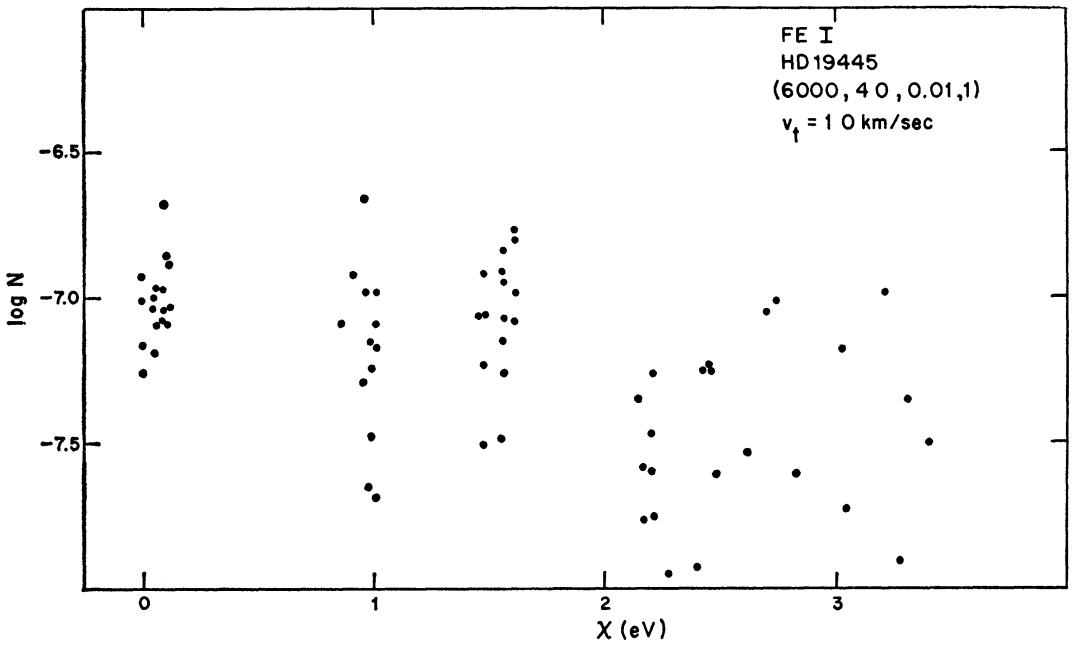

FIG. 3.—Deduced abundance for Fe I lines as a function of the lower excitation potential in HD 19445 for a model (6000, 4.0, 0.01, 1).

for HD 140283 would appear to be log $g \sim 3.3$. This seems a rather low value of surface gravity for a G subdwarf.

A check on the lower limit to log g for HD 140283 can be obtained from its measured proper motion and radial velocity. In order that HD 140283 remain gravitationally bound to the Galaxy,

$$\log g \gtrsim 3.1 .$$

This follows from the observed V magnitude and the upper limit on the distance (luminosity) placed by the computed space velocity. In calculating the space velocity we have arbitrarily varied the distance, ignoring the measured parallax for HD 140283, $\pi = 0''.031$. Large errors in such small parallaxes are quite common. It is therefore reasonable to assume that HD 140283 is an evolved "subdwarf." From Iben's tracks, an age of $\sim 12 \times 10^9$ years can be deduced if log g is as low as 3.1.

A model having (5500, 3.3, 0.01, 2–3) would provide the best compromise within the limits of $T_{\rm eff}$ and log g set by the scans and the space velocity, respectively. However, the difficulties that appear in the abundance versus χ plots and in determining the proper ionization equilibrium are not entirely removed with any model choice.

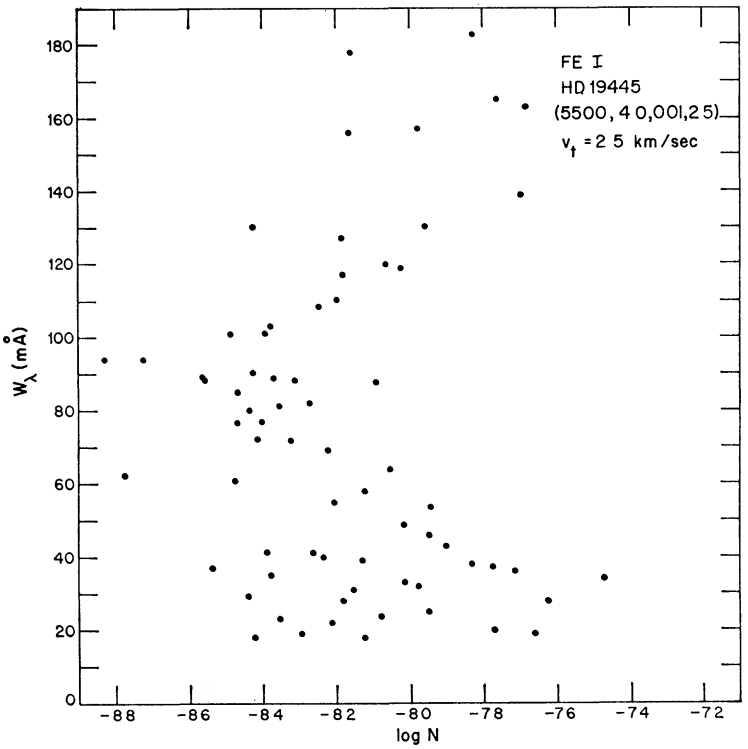

FIG. 4.—Deduced abundance as a function of equivalent width for Fe I lines in HD 19445 for a model (5500, 4.0, 0.01, 2.5).

TABLE 3

IONIZATION EQUILIBRIUM IN HD 140283

Element	No of Lines	Model I (5500, 3 7, 0 01, 0)	Model II (5750, 3 7, 0 01, 0)	Model III (5500, 3 3, 0 01, 0)	Model IV (5500, 3 3, 0 01, 1)	Model V (5100, 3 3, 0 01, 0)
Fe I	75	−7 72	−7 46	−7.71	−7 86	−8 16
Fe II	8	−7 28	−7 24	−7 45	−7 49	−7.52
Ti I .	3	−9 43	−9 16	−9 42	−9 46	−9 87
Ti II .	17	−9 32	−9 25	−9.46	−9 59	−9 67

TABLE 4

IONIZATION EQUILIBRIUM IN HD 19445

Element	No. of Lines	Model I (5500, 4.0, 0 01, 1.0)	Model II (6000, 4 0, 0 01, 1 0)	Model III (5500, 4 0, 0 01, 2 5)
Fe I	69	−7.78	−7 21	−8 17
Fe II	7	−7 34	−7 25	−7 42
Ti I	3	−9 41	−8 92	−9 51
Ti II	13	−9.23	−9 01	−9.52

It should be noted here that for the Sun we find good agreement between the Fe I and Fe II abundances by using the 1964 Utrecht model of the solar photosphere. This suggests that there are no serious errors in the relative values of the Fe I and Fe II f values that we adopted from Corliss and Warner (1964) and Warner (1964). Hence we cannot attribute our difficulties in matching Fe I and Fe II abundances to inaccurate transition probabilities. Moreover, the values of T_{eff} chosen for both stars on the basis of the spectral lines alone would appear to be higher than those predicted from the continuum scans.

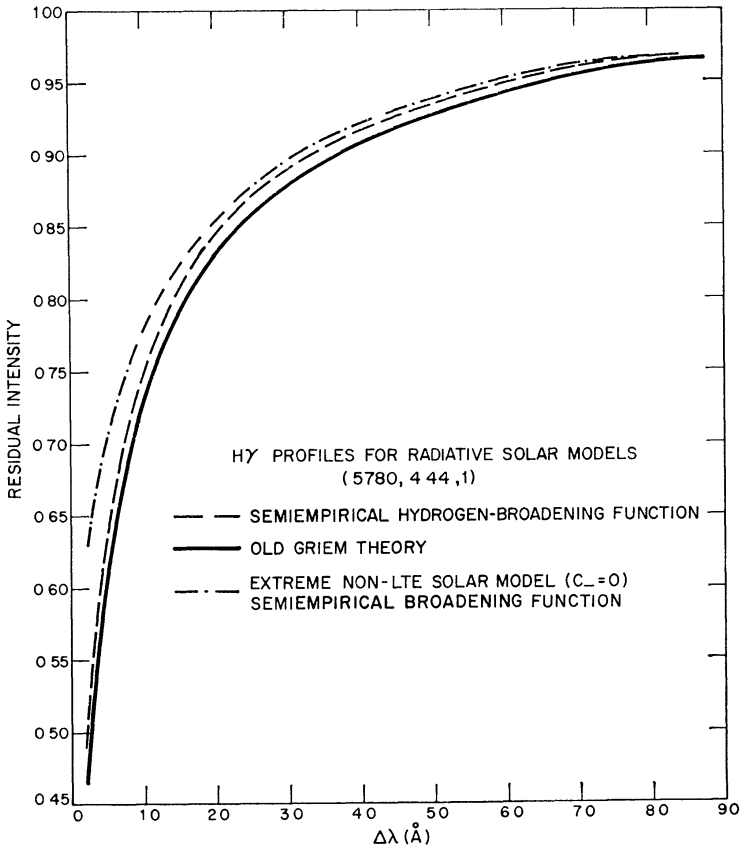

FIG 5 —Comparison of Hγ profiles of a solar model (5780, 4 44, 1) using various line-broadening theories and an extreme non-LTE model. We wish to thank Mr. Deane Peterson of Harvard for computing the semi-empirical case.

This discrepancy is in the same direction as the disagreement between the T_{eff} values determined from the hydrogen profiles and the (lower) T_{eff} values deduced from the continuum scans as reported in Paper I. For Hγ, this effect cannot be explained by invoking departures from LTE or errors in the line-broadening theory as can be seen in Figure 5. Here we plot Hγ profiles computed for a set of (5780, 4.44, 1, 0) models. The "semi-empirical" profile has been calculated using the suggested broadening theory of Edmonds, Schlüter, and Wells (1967); the "Old Griem" profile was computed using the broadening theory of Griem (1960, 1962); the extreme non-LTE solar model was computed under the assumption that the rate of collisional destruction and creation of H^- (C_-) is 0. These computed profiles all agree to within about 2 per cent in the wings, whereas the observed discrepancy is considerably greater.

As a possible mechanism for explaining these inconsistencies, let us consider the role

of convection in subdwarf atmospheres. We should note here the suggestion of Krishna Swamy (1966) that convection plays an important role in determining the temperature structure of Groombridge 1830, a subdwarf having a lower $T_{\rm eff}$ ($\sim$5000° K) than the two stars under examination here. The equation of hydrostatic equilibrium can be written

$$\frac{dp}{d\tau} = \frac{g}{\bar{\kappa}}. \tag{1}$$

With H^- as the primary opacity source we can write

$$\bar{\kappa} = \alpha p_e \phi(T), \tag{2}$$

where α is the cross-section per H^- atom, p_e the electron pressure, and $(\phi)T$ a function of temperature, the exact form of which follows from the H^- Saha equation. Where metals provide the primary source of electrons, we note that

$$p_e \sim Ap, \tag{3}$$

with A being the metal-to-hydrogen ratio. We can now rewrite equation (1) as

$$\frac{p dp}{d\tau} = \frac{(\text{Const.})\, g}{A\phi(T)}.$$

Hence as A decreases, as is the case for subdwarfs, p increases at a given τ. If H^- is the sole opacity source, the *temperature*–optical depth relation is independent of the hydrostatic equilibrium equation since the pressure dependence is absorbed into the definition of the optical-depth variable. Moreover, the differences of radiative and adiabatic gradients, and therefore the convective velocities, are virtually the same for solar-A models and models having A decreased by a factor of 100. Hence the convective flux must be higher in the subdwarf owing to the higher density.

Therefore, we expect that, qualitatively, the temperature gradient in the subdwarf will be reduced compared with a Population I star owing to the increased importance of convective energy transport.

In order to estimate the maximum role played by convection in influencing the line spectrum, we have used the models computed by Swihart and Fischel (1961), which we henceforth denote as "SF" models. They assume that the T-p relation is specified by the adiabatic law in all regions where the Schwarzschild criterion predicts convective instability. Such an assumption of course overestimates the influence of convection.

We have used SF "adiabatic" models to compute Hγ profiles. These profiles were then compared with those computed from radiative models having approximately the same continuum slope in the region 4000 to 6000 Å. The resulting profiles are shown in Figure 6*a*. In Figure 6*b* we reproduce the comparison between the observed Hγ profiles for HD 140283 and HD 19445 and two profiles predicted from radiative models having the indicated parameters. Comparison of Figures 6*a* and 6*b* suggests that the predictions of the SF adiabatic models would reduce the discrepancy between the observed and computed Hγ profiles.

Unfortunately, Swihart and Fischel do not properly calculate the behavior of T and p in the transition region between the regions of radiative and convective energy transport. However, Mihalas (1965) and Latham (1964) have performed more sophisticated treatments in which the run of physical variables in this transition region is computed. Regrettably, only a few such models are yet available. In Figure 7 we sketch the behavior of the temperature-pressure relationship as computed by Mihalas for radiative and convective models.

The "hump" in the transition region is of some significance in discussing the N versus

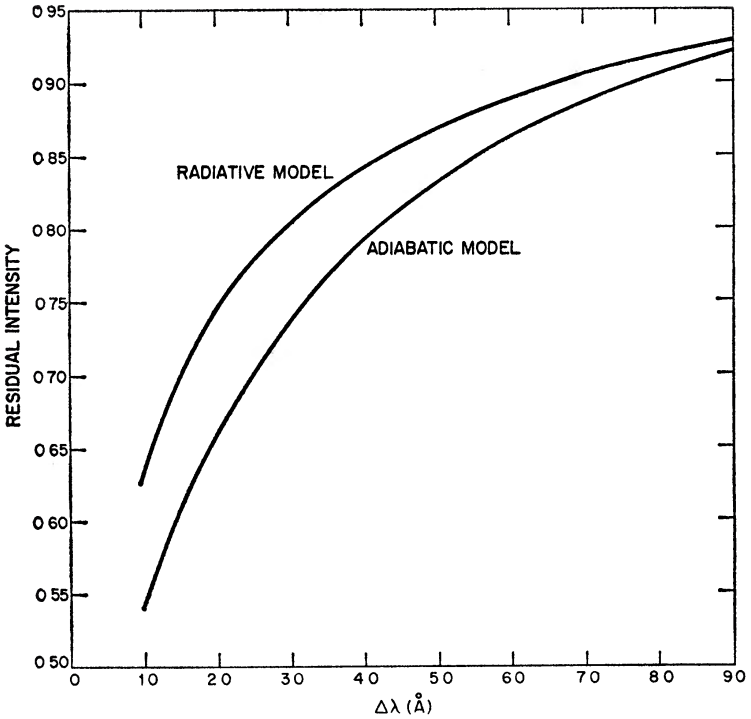

FIG. 6*a*.—Hγ profiles from a radiative model having $T_{\text{eff}} = 6300°$ K as compared with an adiabatic model having $T_{\text{eff}} = 7200°$ K computed by Swihart and Fischel (1961). Both models have approximately the same flux in the visual.

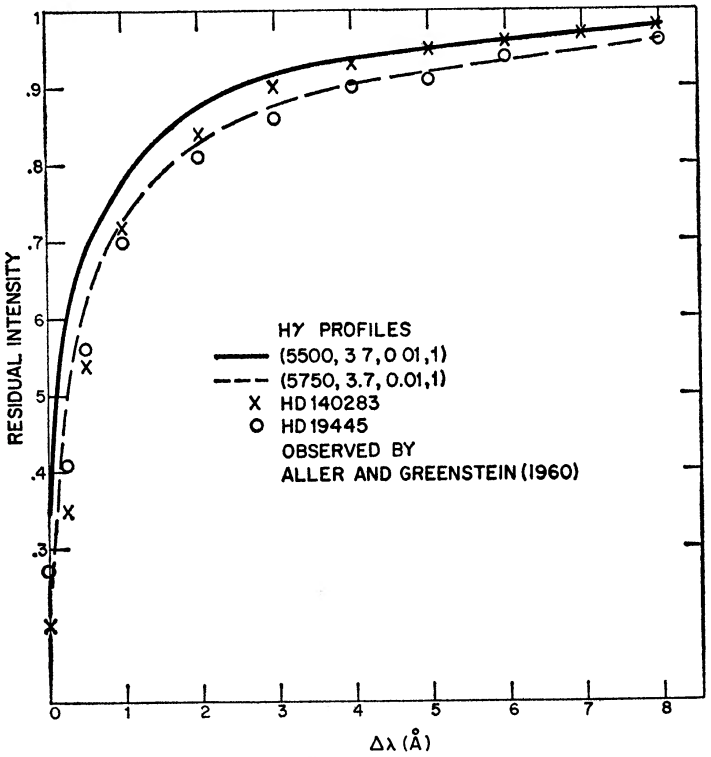

FIG. 6*b*.—Observed Hγ profiles (Aller and Greenstein 1960) for HD 19445 and HD 140283 compared with radiative models of the indicated parameters.

χ plots and the Fe I and Fe II ionization equilibrium. The Fe I lines with $\chi = 3$ are formed between Rosseland optical depths 0.5 and 1, as are most of the Fe II lines. The Fe I lines with $\chi < 3$ are formed higher up in the model. We note from Tables 3 and 4 that the change of Fe II abundance with temperature is small, whereas

$$\frac{\Delta \log N}{\Delta T} \approx \frac{0.1}{100^\circ \text{ K}}$$

for Fe I lines. We suggest that both the Fe I lines with $\chi = 3$ and the Fe II lines are formed in the region of the hump of Figure 7. In the hump, T is increased and hence we must (*a*) increase the computed abundance for the Fe I, $\chi = 3$ lines, and (*b*) decrease the computed abundance for the Fe II lines.

It would be desirable, of course, to present detailed arguments that would allow more quantitative evaluations of our suggestion of the increased role of convection in subdwarfs. But unfortunately, the present status of convective-atmosphere computations does not permit such a discussion at this time. We are currently investigating the effects of convection in subdwarf atmospheres in conjunction with T. Dennis of Princeton University.

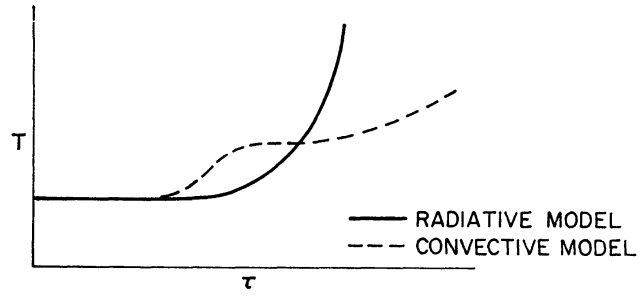

FIG. 7.—Comparison of radiative and convective temperature structures for the same T_{eff} after Mihalas (1965).

The arguments presented above suggest that the difference in temperature between radiative and convective models appropriate to HD 140283 may be as large as 250° K near optical depth $\tau = 1$. We have therefore chosen to compute the abundances from two radiative models: Model VI (5500, 3.7, 0.01, 1) and Model II (5750, 3.7, 0.01, 0). Model VI is most likely correct in the outer layers, while Model II adequately represents the deeper layers of the line-forming region.

Although our analysis indicates $2 < v_t < 3$ km/sec for HD 140283 and $1 < v_t < 2$ km/sec for HD 19445, uncertainties in our temperature structure may affect our choice of v_t. Despite these uncertainties, we feel sure that $v_t > 0$ for both stars. The values of microturbulent velocity $v_t \sim 0$ deduced in previous work may result from the assumption implicit in differential curve-of-growth analyses, namely, that the temperature structure of the subdwarf is identical to that of the Sun. This is certainly not the case, since the line and bound-free metal opacities are significantly more important in the Sun.

III. TECHNIQUE OF ABUNDANCE DETERMINATIONS

In computing the abundances of all elements the method described by Strom, Gingerich, and Strom (1966) was used. Their procedure makes use of model atmospheres to compute the line opacity and source function as a function of optical depth for a given trial abundance. The line profile and equivalent width are then computed, and the equivalent width is compared with the observed value. The abundance is varied until a match between observed and calculated equivalent widths is achieved.

In our analysis of both stars we used the equivalent widths of Aller and Greenstein (1960). The lowest dispersions used in their work were 10 Å/mm, and their spectra, we feel, represent the best available equivalent-width measurements for subdwarfs. The results of our analysis are summarized in Table 5, in which we give for our choice of "best" model atmospheres the values of log ($N_{el}/N_{Fe\ I}$) and the standard deviation in the mean of that abundance determination. By presenting the abundances relative to

TABLE 5

HD 140283 AND HD 19445 ABUNDANCES

Element	HD 140283 Model VI	HD 140283 Model II	No Lines	HD 19445 Model I	HD 19445 Model II	No Lines	GMA
Fe I	0 0	0 0	75	0 0	0 0	69	0 0
Fe II	+0 74±0 24	+0 22±0 23	7	+0 44±0 10	−0 04±0 10	7	
Ti I	−1 40± 45	−1 70± 41	3	−1 63± 10	−1 71± 01	3	−1 89
Ti II	−1 37± .12	−1 79± 11	17	−1 45± 11	−1 80± 12	13	
Cr I	−1 36± 17	−1 48± 07	3	−1 36± 30	−1 36± 30	2	−1 21
Cr II	−0 19	−0 71	1	−0 90	−1 47	1	
Ca I	−0 12± 18	−0 30± 36	4	−0 06± 12	−0 30± 14	7	−0 42
Ca II	+0 70	+0 21	1				
Ni I	−0 31± 11	−0 87± 11	5	−1 70± 13	−1 32± 16	4	−1 06
Mg I	+1 54± 30	+1 16± 30	5	+1 49± 21	+1 64± 17	4	+0 83
Co I	−1 95	−1 87	1	−1 21	−1 04	1	−1 93
Si I	+1 19	+1 06	1	+1 52	+1 50	1	+0 93
Al I	−1 42± 29	−0 85± 26	2	−0 49± 80	−0 28± 58	2	−0 37
Mn I	−1 74± 08	−1 79± 09	2	−1 36± 46	−1 31± 47	2	−1 67
Sc II	−3 36± 19	−3 79± 20	2	−3 39± 15	−3 69± 09	2	−3 75
Zr II	−3 25	−3 60	1				−4 34
La II	−2 63	−3 04	1				−5 17
Y II	−4 22± 37	−4 56± 35	2	..		.	−4 17
Ba II	−5 15	−5 51	1	−4 57	−4 76	1	−4 47
Corliss-Bozman *gf* values:							
Sr II	−3 15	−3 25± 14	2	−2 79± 13	−2 96± 08	2	−3 97
Bates-Damgaard *gf*							
Sr II	−4 15	−4 25± 27	2	−3 74± 05	−3 95± 04	2	−3 97
Fe I ($\log N_{Fe\ I}/N_H$)	−1 93± 3	−1 45± 3	..	−2 55	.. ..		0 0*
C (CH bands)	−8 10±0 15	−7 46±0 16	75	−7 78±0 20	−7 21±0 10	69	−5 43

* For carbon, the abundances for each model are log ($N_*/N_\odot$)

Fe I, we minimize the effect of the uncertainty of our determination of microturbulent velocity. We note that a change of 1 km/sec in v_t introduces a maximum change of 0.4 in the absolute abundance of Fe I, but only about 0.2 in the relative abundances of most elements. Larger changes in the relative abundance may occur for elements whose lines all lie near the weak-line portion of the curve of growth.

We should note that the zirconium and lanthanum abundances are each deduced from only one weak and possibly blended line. It is quite probable that the abundances we deduce for these important *s*-process elements are spurious.

The carbon abundances were computed using lines arising from the (0,0) CH band in the following way. We first computed the number density of the CH molecule, N_{CH}, as a function of optical depth for each of our model atmospheres. The method and numerical constants used for computing N_{CH} have been described by Dolan (1965).

His computer program, kindly loaned to us, computes simultaneously the number density of fifty-nine molecules, given the relative abundances of the major atmospheric constituents. We next determine the fraction of all CH molecules in each rotational level by using molecular constants for CH tabulated by Herzberg (1950) and Gerö (1941). The transition probabilities S_K as a function of K (the rotational quantum number) were obtained from Schadee (1964), who assumed both levels correspond to Hund's case *b*, which is valid for high-rotational quantum numbers. The value of $f_{el}f_{00}$, the product of electronic and vibrational transition probabilities, was chosen to be 10^{-3}. Since all the lines arising from CH are weak, the value of $f_{el}f_{00}$ enters linearly into the abundance determination, and unfortunately, it is entirely possible that this value is in error

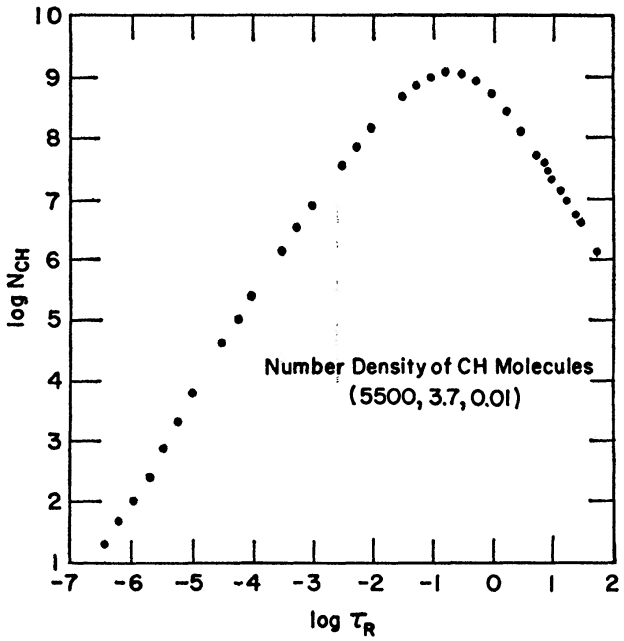

FIG. 8.—Number density of CH molecules plotted against Rosseland optical depth for the indicated model atmosphere. The program of Dolan (1965) was used in the computations.

by as much as a factor of 5. Moore and Broida's (1959) tables were used to identify the K values for each observed line. We then computed the line-absorption coefficient

$$\kappa_\nu{}^l = \frac{\sqrt{(\pi)}\, e^2}{m\, c} f_{el} f_{00} \frac{S_K}{2K+1} \frac{H(a,v)}{\Delta\nu_D} N_{(0,0,K)} (1 - e^{-h\nu/kT})$$

as a function of optical depth. Here, K is the rotational quantum number; $H(a,v)$, in the usual notation, is the Voigt function; $\Delta\nu_D$ is the Doppler width; and $N_{(0,0,K)}$ is the number of molecules in the Kth rotational state per gram of stellar material. At temperatures near 5500° K, N_{CH} is strongly dependent on temperature. In fact, a change of 500° K changes N_{CH} by a factor of 5. Thus the choice of T_{eff} for the star will significantly affect the deduced carbon abundance. Aller and Greenstein (1960) obtained a carbon abundance a factor of 10^3 less than the solar value, that is, a factor of 10 less than the iron-abundance deficiency for both these stars. However, they chose temperatures of 4500° K for HD 19445 and 4230° K for HD 140283 as representative of the layers in which the CH lines were formed. In Figure 8 we plot N_{CH} against optical depth for a (5500, 3.7, 0.01) model, and we find that N_{CH} peaks sharply at $\tau \sim 0.1$, which corresponds to $T \sim 5000°$ K. If, as is done in Aller and Greenstein, a single-layer approxi-

mation is used, one should therefore choose a temperature of about 5000° K. Since Aller and Greenstein chose too low a value of T, they obtained too high a value of N_{CH} and thus predicted too small a carbon abundance. Danziger (1966) has found deficiencies in the carbon abundance as deduced from curve-of-growth analyses of CH lines in ζ^1 Ret and γ Pav. He assumes that the temperature of CH line formation corresponds to the boundary temperature. Thus his carbon abundances may be too low for the same reason as we found for Aller and Greenstein's work on HD 19445 and HD 140283.

As a further check on the molecular parameters used in our analysis we have computed the abundance of carbon in the Sun using the observed strengths of the (0,0) band CH lines taken from Hunaerts (1947). The Utrecht reference model (Heintze, Hubenet, and de Jager 1964) was used as the model solar atmosphere. We obtained log $N_C/N_H = -3.06$, which compares with log $N_C/N_H = -3.28$ obtained from the C I lines. We consider this agreement entirely satisfactory. The only comment we are able to make, given the observational uncertainties, is that the carbon deficiency is probably not different from the element deficiencies for the other constituents. Our conclusions agree with Baschek's (1962) for HD 140283. However, his result is based on a model for which T_{eff} is probably too high and hence does not represent independent

TABLE 6

AVERAGE ABUNDANCES FOR PROCESSES OF NUCLEOSYNTHESIS

log $N_*/N_\odot$	HD 140283		HD 19445	
	Model I	Model II	Model I	Model II
α-process	−2 09	−1 84	−1.82	−1 28
e-process	−2 20	−1 99	−2.26	−1 75
s-process	−2 64	−2 48	−2 26	−1 81
Sr, Y, Ba only	−2 74	−2 60	−2 29	−1 92

confirmation of our results. We also note that the deduced carbon abundance is much more accurate for this star, since more CH lines are observed in this, the cooler of the two subdwarfs; only one of the nine CH lines or blends observed by Aller and Greenstein (1960) in HD 19445 was suitable for analysis, and it was a blend of two components (Q_{1d} and Q_{2d} for $K = 22$). Five lines were used for HD 140283, one of which was a blend.

For Sr II and Ba II, the Bates-Damgaard transition probabilities were used in preference to the Corliss-Bozman (1962) experimental determinations, which appear to be too low by as much as a factor of 8 (see Garstang and Hill 1966).

Nickel presents further problems, in that the absolute calibration of the transition probabilities used by us (those of Corliss 1965) differs greatly from those used in the GMA study. In view of these more recent gf-value determinations we have reduced the GMA nickel abundance by 0.4 in the log. The problem of the solar nickel abundance has also been discussed recently by Cowley (1966), who arrives at similar conclusions.

Since the GMA study did not include lanthanum and yttrium, we have used as "standard" the abundances given in Allen (1963).

IV. BRIEF DISCUSSION OF RESULTS

If we ignore the highly uncertain zirconium- and lanthanum-abundance determinations, we note a general trend in HD 140283 for elements formed by slow neutron capture, strontium, yttrium, and barium, to be deficient relative to the e-process elements. To support this impression, we present in Table 6 the average deficiency compared to

solar abundances for the α-process, e-process, and light and heavy s-process elements. In HD 19445, only the α-process elements appear to be enhanced. However, it might conceivably be argued from our data that within the uncertainties of each abundance determination there is no difference in the relative abundances of the elements.

Moreover, we note that the abundance deduced from Mn is normal for both stars in contradiction to Wallerstein's (1962) results for his subdwarfs. Danziger (1966) and Aller and Greenstein (1960) also do not find excessive Mn deficiencies.

Perhaps the most significant result of this analysis is the reconfirmation of the existence of element deficiencies amounting to factors of 40 and 200 in two very old members of the Galaxy.

Part of this research was supported by contract NGR 22-024-001 from the National Aeronautics and Space Administration.

REFERENCES

Allen, C W. 1963, *Astrophysical Quantities* (2d ed.; London: Athlone Press).
Aller, L H , and Greenstein, J. L. 1960, *Ap. J. Suppl* , **5,** 139.
Baschek, B. 1959, *Zs. f Ap* , **48,** 95.
———. 1962, *ibid.*, **56,** 207.
Chamberlain, J. W., and Aller, L. H. 1951, *Ap J.*, **114,** 52.
Corliss, C. H. 1965, *N.B S. J. Res.*, **69A,** 87.
Corliss, C H., and Bozman, W. R. 1962, *N.B.S Mong. 53*
Corliss, C. H., and Warner, B. 1964, *Ap. J. Suppl* , **8,** 395.
Cowley, C. R. 1966, *Ap. J.*, **143,** 352.
Danziger, I. J. 1966, *Ap J* , **143,** 527.
Dolan, J. F. 1965, *Ap J.*, **142,** 564.
Edmonds, F. N , Schlüter, H., and Wells, D. C. 1967, *Mem. R A S.*, **71,** 271.
Faulkner, J , and Iben, I., Jr. 1966, *Ap. J* , **144,** 945
Garstang, R. H., and Hill, S. J. 1966, *Pub. A S P.*, **28,** 70.
Gerö, L 1941, *Zs. f. Phys.*, **118,** 27.
Goldberg, L., Müller, E A., and Aller, L. H. 1960, *Ap. J. Suppl* , **5,** 1.
Griem, H. R. 1960, *Ap. J.*, **132,** 883.
———. 1962, *ibid* , **136,** 422.
Heintze, J. R. W., Hubenet, H , and Jager, C de 1964, *Smithsonian Ap. Obs. Spec Rept No 167*, p 239.
Herzberg, G. 1950, *Molecular Spectra and Molecular Structure*, Vol. 1: *Spectra of Diatomic Molecules* (New York: D. Van Nostrand Co.).
Hunaerts, J. 1947, *Ann. d'ap.*, **10,** 237.
Krishna Swamy, K. S. 1966, *Ap. J.*, **145,** 174.
Latham, D. W. 1964, *Smithsonian Ap. Obs. Spec. Rept. No. 167*, p. 199.
Melbourne, W. G. 1960, *Ap. J.*, **132,** 101.
Mihalas, D. 1965, *Ap J* , **141,** 564.
Moore, C. E , and Broida, H. P. 1959, *N.B.S. J. Res* , **63A,** 19.
Oke, J. B. 1965, *Ann. Rev. Astr. and Ap.*, **3,** 23.
Schadee, A. 1964, *B.A N.*, **17,** 311.
Strom, S. E. 1967, *Ap. J.*, **150,** 637.
Strom, S. E , Cohen, J. G., and Strom, K. M. 1966, *Ap. J.*, **147,** 1038.
Strom, S. E., Gingerich, O. J., Strom, K. M. 1966, *Ap. J.*, **146,** 880.
Swihart, T. L., and Fischel, D. 1961, *Ap J. Suppl.*, **5,** 291.
Wallerstein, G. 1962, *Ap. J. Suppl.*, **6,** 407.
Warner, B. 1964 (private communication).